

# Assessing ecological exposure from utility-scale wind and solar expansion: a global integrity-conditioned framework for environmental management

Journal: Environmental Management

Author: Magdalena Olczyk

Affiliation: Faculty of Management and Economics, Gdańsk University of Technology, Gdańsk, Poland

Corresponding author email: Magdalena.Olczyk@pg.edu.pl

## Online Resource 1

### S1. Data Sources and Versions

**Table S1.** Data sources and versions used in the analysis.

Dataset	Version / Release	Spatial Resolution	Format Used	License / Access
Global Renewables Watch (Solar & Wind)	Q2 2024	Asset-level (polygons & points)	GeoPackage (.gpkg)	Open data (MIT-style distribution)
Global Human Modification (gHM)	Version 1 (2019)	~1 km raster	GeoTIFF (.tif)	NASA SEDAC open access
Human Footprint	LWP-3 (2009, 2018 release)	~1 km raster	GeoTIFF (.tif)	NASA SEDAC open access
World Database on Protected Areas (WDPA)	2024 release	Polygon (global)	Shapefile (.shp)	Free for research; redistribution restricted
GADM Administrative Boundaries	Version 4.1	Polygon (multi-level)	GeoPackage (.gpkg)	Academic use; redistribution restricted

*All datasets are publicly accessible from the original providers. Derived indicators and processing scripts necessary to reproduce the analysis will be made available upon publication.*

### S2. Scale–Siting Decomposition Tables (Fig. 2)

**Table S2.** Panel A – gHM baseline integrity

Quadrant	n	% obs	$\Delta A$ (km <sup>2</sup> )	% $\Delta A$	$\Delta A \times I$ (km <sup>2</sup> )	% $\Delta A \times I$	$\Delta A \times (1-I)$ (km <sup>2</sup> )	% $\Delta A \times (1-I)$
High-scale / High-integrity	29	24.4%	33.508	83.7%	26.776	93.4%	6.732	59.1%
High-scale / Low-integrity	27	22.7%	5.290	13.2%	1.324	4.62%	3.966	34.8%
Low-scale / High-integrity	31	26.1%	0.578	1.44%	0.391	1.36%	0.187	1.65%
Low-scale / Low-integrity	32	26.9%	0.669	1.67%	0.166	0.58%	0.503	4.41%
Total	119	100.0%	—	100.0%	—	100.0%	—	100.0%

**Table S3.** Panel B – Human Footprint baseline integrity

Quadrant	n	% obs	$\Delta A$ (km <sup>2</sup> )	% $\Delta A$	$\Delta A \times I$ (km <sup>2</sup> )	% $\Delta A \times I$	$\Delta A \times (1-I)$ (km <sup>2</sup> )	% $\Delta A \times (1-I)$
High-scale / High-integrity	41	31.8%	35.784	82.5%	32.153	87.8%	3.630	53.7%
High-scale / Low-integrity	24	18.6%	6.314	14.6%	3.588	9.80%	2.726	40.3%
Low-scale / High-integrity	24	18.6%	0.518	1.20%	0.458	1.25%	0.061	0.90%
Low-scale / Low-integrity	40	31.0%	0.753	1.74%	0.406	1.11%	0.348	5.14%
Total	129	100.0%	—	100.0%	—	100.0%	—	100.0%

### S3. Robustness Checks

Indicators are recomputed under alternative integrity layers (gHM vs Human Footprint) and nonlinear weighting exponents ( $\gamma = 2, 3$ ) for RIEPI, and under alternative upper-tail thresholds ( $q = 0.80, 0.95$ ) for RLHIPI. Table S4 summarizes ranking instability relative to the baseline specification.

Ranking instability is reported as  $|\Delta rank| = |rank_{alt} - rank_{base}|$  together with Spearman rank correlations. Rankings use 2017–2024 totals (descending order; 1 = highest exposure) and the “min” tie rule. RLHIPI robustness is evaluated on the subset of countries with non-zero RLHIPI under at least one threshold to avoid tie-driven rank noise. Additional pre-specified tests that require reprocessing of footprint geometries (wind buffer radii) or alternative quantile definitions (deployment-conditioned and global quantiles) follow the same workflow and can be regenerated from the spatial pipeline.

**Table S4.** Ranking robustness summary (country-level).

Specification	N	Median   $\Delta rank$	Mean   $\Delta rank$	Max   $\Delta rank$	Spearman $\rho$	% reclassified
<b>Panel A: RIEPI robustness (baseline: gHM, <math>\gamma = 1</math>)</b>						
HFP layer ( $\gamma=1$ )	40	2	2.0	11	0.97	82.5
$\gamma=2$ (gHM)	40	2	2.3	9	0.96	85.0
$\gamma=3$ (gHM)	40	2	4.0	20	0.86	75.0
HFP, $\gamma=2$	40	3	4.2	11	0.89	90.0
HFP, $\gamma=3$	40	4	6.0	19	0.75	92.5
<b>Panel B: RLHIPI robustness (baseline: <math>q = 0.90</math>)</b>						
$q=0.80$ (vs 0.90)	10	0	0	0	1.00	0.0
$q=0.95$ (vs 0.90)	10	1	1.1	2	0.72	100.0

*RIEPI rankings remain highly correlated across moderate specification changes, while stronger non-linear weighting produces larger reordering. RLHIPI rankings are stable under modest threshold variation and shift primarily when the tail definition is tightened to the extreme tail ( $q = 0.95$ ).*

#### S4. Country hotspot summaries

**Table S5** reports the countries with the highest cumulative integrity-conditioned exposure under the baseline gHM specification for 2017–2024. Fig. S1 maps the same cumulative country-level surface and pairs it with a top-country ranking. For plotting only, country boundaries follow the Natural Earth low-resolution layer; the table retains the full analytic country list used in the indicator calculations.

**Table S5.** Top country exposure hotspots by cumulative RIEPI (gHM baseline, 2017–2024).

Rank	Country	Cum. $\Delta A$ ( $km^2$ )	Cum. RIEPI ( $km^2\text{-eq}$ )	Footprint rank	Shift	Peak RLHIPI $q_{0.90}$	Peak year
1	Mexico	8.35	3.75	2	+1	1.00	2018
2	Chile	22.94	2.20	1	-1	0.36	2022
3	Israel	1.13	0.88	5	+2	0.00	—
4	Japan	0.78	0.70	7	+3	0.00	—
5	Turkmenistan	0.81	0.53	6	+1	0.00	—
6	Jamaica	0.44	0.36	9	+3	0.00	—
7	Armenia	0.60	0.20	8	+1	0.00	—
8	Cyprus	0.24	0.19	15	+7	0.00	—
9	Kuwait	0.36	0.18	11	+2	0.00	—
10	Russia	0.32	0.18	12	+2	0.00	—

*Positive shift values indicate that a country moves upward in the exposure ranking when footprint growth is conditioned on baseline integrity.*

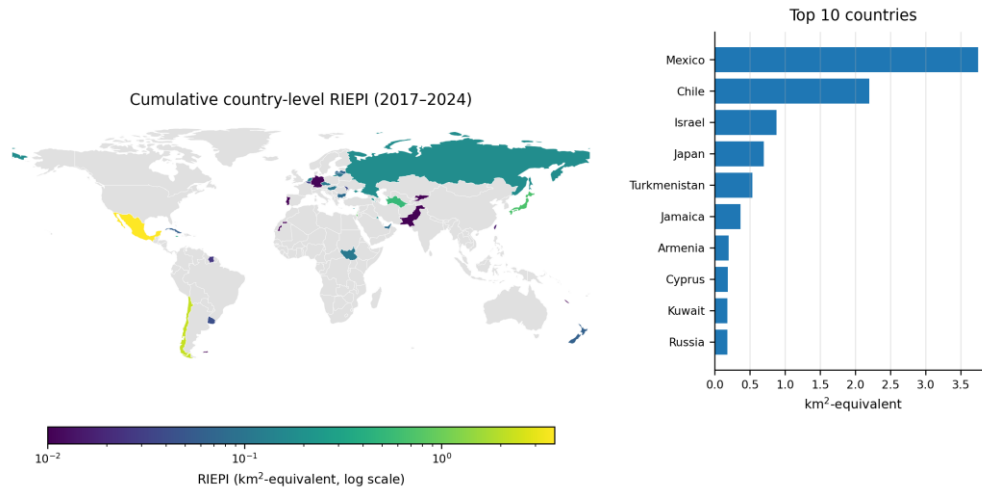


**Fig. S1.** Country hotspot map and top-country ranking for cumulative RIEPI (gHM baseline, 2017–2024). The map uses a logarithmic color scale to improve visibility outside the highest-exposure cases.

### S5. Regional hotspot summaries

**Table S6** reports the regional units with the highest cumulative RIEPI over 2017–2024. The regional ranking shows that aggregate country-level exposure is anchored in a small set of repeatedly observed subnational units rather than being evenly distributed across space.

**Table S6.** Top regional exposure hotspots by cumulative RIEPI (gHM baseline, 2017–2024).

Rank	Region	Country	Cum. $\Delta A$ (km <sup>2</sup> )	Cum. RIEPI (km <sup>2</sup> -eq)	Shift	Peak RLHIPI q0.90	Peak year
1	Aguascalientes	Mexico	8.35	3.75	+1	1.00	2018
2	Antofagasta	Chile	22.94	2.20	-1	0.36	2022
3	Golan	Israel	1.13	0.88	+2	0.00	—
4	Aichi	Japan	0.78	0.70	+4	0.00	—
5	Aşgabat	Turkmenistan	0.81	0.53	+1	0.00	—
6	Ahal	Turkmenistan	0.81	0.53	+1	0.00	—
7	Clarendon	Jamaica	0.44	0.36	+3	0.00	—
8	Aragatsotn	Armenia	0.60	0.20	+1	0.00	—
9	Famagusta	Cyprus	0.24	0.19	+7	0.00	—
10	Al Ahmadi	Kuwait	0.36	0.18	+2	0.00	—

*Peak RLHIPI q0.90 reports the largest annual upper-tail exposure share observed for each region in the baseline tail specification.*

### S6. RLHIPI hotspot persistence across thresholds

**Fig. S2** plots every country-year observation with positive RLHIPI under at least one threshold ( $q = 0.80, 0.90, \text{ or } 0.95$ ). The plot highlights whether country-year tail hotspots persist or disappear as the tail definition is tightened. RLHIPI should therefore be interpreted as a concentration diagnostic for exposure in the highest-integrity fraction of landscapes, not as a direct estimate of realized biodiversity outcomes.

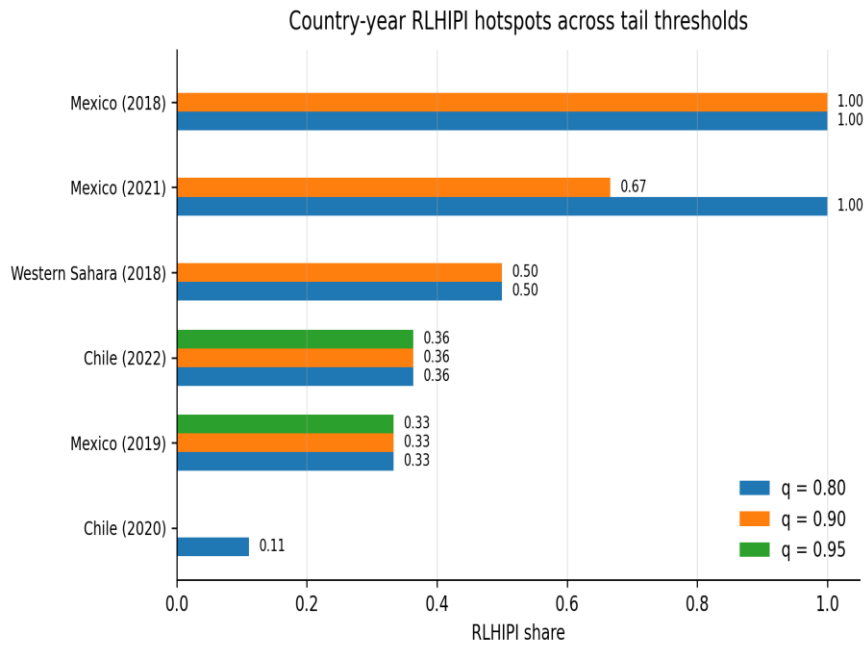


**Fig. S2.** Country-year RLHIPI hotspots across  $q = 0.80, 0.90,$  and  $0.95$ . Only observations with positive RLHIPI under at least one threshold are shown.